

Search for Heavy, Long-Lived Particles that Decay to Photons at CDF

CDF Collaboration

Abstract

We present the results of a search for heavy, long-lived particles that decay to photons in a sample of $\gamma + \cancel{E}_T + \text{Jet}$ events at CDF Run II. Candidate events are selected based on the delayed arrival time of the photon at the calorimeter as measured with the a new timing system that was recently installed on the electromagnetic calorimeter. We find 10 events using 570 pb^{-1} of data to be consistent with the background estimate of 7.6 ± 1.9 events. We show exclusion regions and set limits on GMSB models with the delayed photons via long-lived neutralinos with the decay mode $\tilde{\chi}_1^0 \rightarrow \gamma \tilde{G}$.

1 Introduction

There is a wide program at the Tevatron to look for the hints of the new physics beyond the Standard Model (SM) which is incomplete [1]. Recently, there is a new focus on models with long-lived particles for theoretical reasons, as well as new advances in the detectors at the Tevatron. Such models [2] predict the existence of heavy, long lived, massive exotic particles such as sleptons or neutralinos to satisfy constraints from cosmic-microwave background and Big-Bang Nucleosynthesis. Another model [3] predicts the interactions with highly displaced vertices as a result of the hidden valleys. Both scenarios give rise to the existence of the photons with delayed time. The Run I observation of the $ee\gamma\gamma\cancel{E}_T$ [4] event hints that the new physics can show up with the photon in the final state.

In this document we present a search for heavy, long-lived particles that decay to photons using the CDF detector in the Tevatron Run II. The final state signature consists of a photon with a delayed arrival time measured by the recently installed calorimeter timing (EMTiming) system [5], one energetic jet, and missing transverse energy (\cancel{E}_T). For concreteness, to study the detector acceptance we use well established supersymmetry model with gauge mediated supersymmetry breaking (GMSB) [4]. In this scenario the lightest neutralino ($\tilde{\chi}_1^0$) is the next-to-lightest supersymmetric particle

(NLSP) which decays into a photon and a gravitino (\tilde{G}), which is the lightest supersymmetric particle (LSP). The neutralino is allowed to have a macroscopic lifetime of the order of $O(1 \text{ ns})$ range. While we use a quasi model-independent (signature-based) approach in our search, we use this model as a benchmark to compare our sensitivity with other searches at LEP [6].

The lifetime of the neutralino is a free parameter in the model, and can be quite large. The GMSB model does not have any constraints on the $\tilde{\chi}_1^0$ lifetime, so it can be significant. The cross section is dominated by gaugino pair production (Figure 1), producing a pair of neutralinos in association with other final state particles that can be identified in the calorimeter, for example, as jets. The \tilde{G} escapes the detector undetected and gives rise to \cancel{E}_T . Depending on whether the neutralino decays inside the detector or not, due to its large decay length, the event can have a signature of $\gamma\gamma\cancel{E}_T$ or $\gamma\cancel{E}_T$ with one or more additional jets. The photons from decays of long-lived neutralinos would appear to be arriving with a delay into the CDF detector as shown in Figure 2 and is described in [7]. The delay is due to the longer path length of the photon if compared to the photons originating at the collision point, hence the name for the search - delayed photons. For concreteness we use the Snowmass Slope constraint (SPS 8) [8] to quote GMSB results as a function of $\tilde{\chi}_1^0$ mass and lifetime.

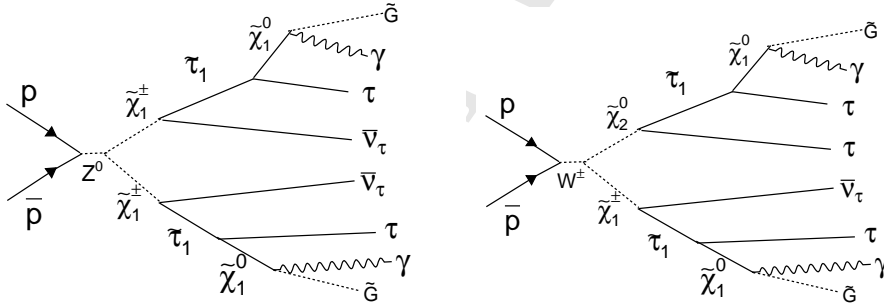


Figure 1: The Feynman diagrams for the two leading GMSB processes. The final state \tilde{G} leaves the detector undetected producing missing transverse energy, \cancel{E}_T . We require a jet that can be either the tau particle decaying either hadronically or electronically, or the second photon. Other processes, such as slepton pair production, can also contribute to the acceptance.

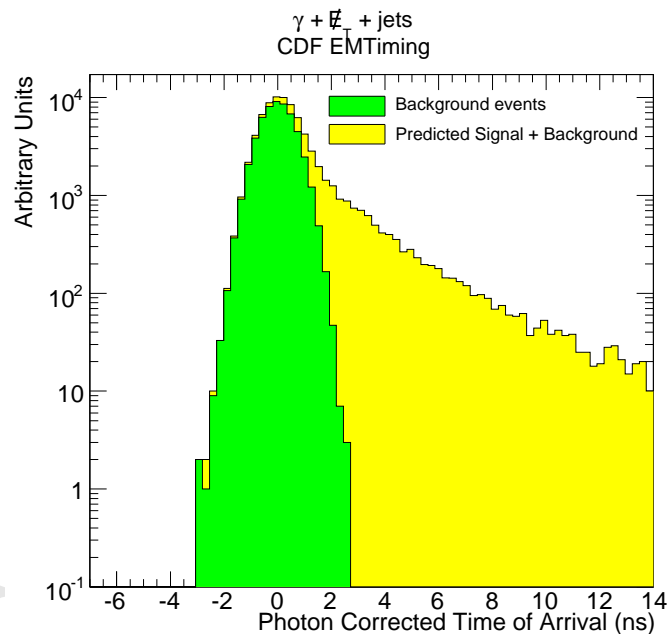
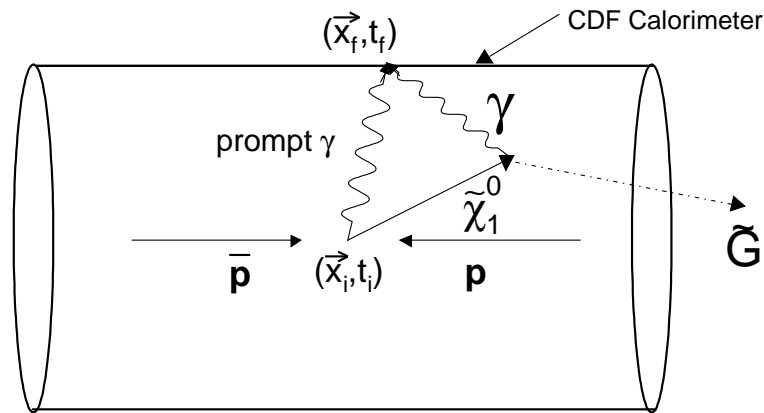


Figure 2: On the top: the decay of the heavy particle into a photon and a gravitino. It takes the photon more time to reach the detector compared to the photon from the collision point. On the bottom: A toy Monte Carlo signal simulation of the Standard Model background and the signal [7]. Green is SM, and is normalized to the expected time of arrival, thus it is zero and smeared by the timing resolution (0.65 ns). The yellow is the signal and is significantly different from zero, as expected from the neutralino decaying in flight.

2 Data Selection

The analysis selection begins with events that pass the CDF trigger by virtue of having a high energy photon-like EM cluster (presumably from our photon) in the central portion of the detector, $|\eta| < 1.1$, and large missing transverse energy, \cancel{E}_T . The trigger is 100% efficient for the final, offline selected γ and \cancel{E}_T energies.

Offline, we select events with γ , \cancel{E}_T , and a jet as shown in Table 1. Only the highest E_T photon is picked, while any second photon candidate would be counted as a jet. In this way we are sensitive to the signatures with one or both neutralinos decaying inside the detector. The selection criteria is shown in Table 1. We apply extra topological cuts to reduce the contamination from QCD events with fake \cancel{E}_T cosmic rays, and beam halo effects. The cut on $\Delta\phi$ between a photon and a leading jet rejects QCD events where a jet is poorly measured and causes \cancel{E}_T . We also require a high $\sum P_T$ good vertex to reduce beam halo and cosmics contamination since they are not correlated with a collision.

The list of all baseline cuts is shown in Table 1. The upper portion cut efficiencies are estimated from data independently from one another, while acceptance numbers in the low part of the table are estimated from signal Monte Carlo and are cumulative. Details about signal Monte Carlo are in Section 4. The final cut on the corrected time of arrival of the photon is also discussed in Section 4 .

Quality Cuts: γ $E_T > 30$ GeV $ \eta < 1.1$	$\epsilon(\%)$
Photon ID and Fiducial	74
Cosmic Rejection:	
$\Delta\phi > 30^\circ$ between γ and trackless μ stub	98
Collision Fiducial	95
Baseline Cuts	
Photon $ \eta < 1.1$ $E_T > 30$ GeV, $\cancel{E}_T > 50$ GeV	41
Good Vertex	40
Jet E_T^{jet} (cone 0.7) > 30 GeV, $ \eta_{\text{detector}}^{\text{jet}} < 2.0$	27
Optimized Cuts	
$\cancel{E}_T > 50$ GeV	19
$\Delta\phi(\cancel{E}_T, \text{Jet}) > 0.5$ rad	18
$1.5 \text{ ns} < t_{\text{arrival}} < 10 \text{ ns}$	7

Table 1: The data selection criteria and the total event efficiency. We note that the top three cuts are estimated from data and should be model-independent. The lower set of cuts are model-dependent and are for an example mass point at $m_\chi = 93.6$ GeV. The efficiency is given cumulatively, as a function of the cuts.

3 Backgrounds

There are two major sources of the backgrounds: collision and non-collision photon candidates. Collision photons are presumed to be from the Standard Model interactions (e.g. $\gamma + j + \text{Fake } \cancel{E}_T$; $jj + \text{Fake } \cancel{E}_T$, j fakes γ ; $W \rightarrow e\nu$, electron fakes γ). The non-collision photon candidates are produced by cosmic rays and beam effects. Cosmic rays are not correlated in time with collisions, and therefore their timing shape, as we will show later, is flat in time. The photon candidates from beam halo have negative time. We use events in the time regions that do not overlap with prompt photons to estimate the overall non-collision backgrounds. All three are estimated using data.

A full description of the EMTiming system as well as its timing resolution and various effects can be found in [5]. The timing distribution shape for collision events is estimated from $W \rightarrow e\nu$ data. It is a double Gaussian centered at zero with the primary RMS=0.64 ns and the secondary RMS=2.05 ns as shown in Figure 3. The collision vertex time is estimated from COT tracks and has an RMS of 1.3 ns. The highest track $\sum P_T$ vertex is always picked as the collision vertex. In the $W \rightarrow e\nu$ events the electron track is dropped from the vertexing to closely mimic events with photons. The double Gaussian can be understood as coming from when the photon timing is associated with the correct primary vertex, and when it is associated with a vertex unrelated to the collision. For more details see [5]. The shape of the distribution does not depend on the kinematic cuts used to select the final sample, but the relative event fraction of right to wrong vertex can vary.

The timing distributions of non-collision photon candidates produced by cosmic rays and beam effects are shown in Figure 3 and are estimated from data using events with no track activity. The cosmic contribution is flat in time and drops near the edges of the energy integration gate. The beam halo photon candidates are produced by the muons flying parallel to the beam line. Relative to the nominal collision time they populate the negative region. Those events normally have a trail of the calorimeter towers with some energy deposited in the same wedge with the photon, the feature used to separate cosmic ray photons from beam halo. We use those shapes as the templates to estimate contributions from each of the backgrounds by fitting them to the events in the time windows not overlapping with the prompt or signal regions.

In order to find the backgrounds in the timing window of [1.5, 10] ns after all cuts we first normalize the non-collision templates to the events in window of [-30, -8] dominated by beam halo, and [30, 80] ns, dominated by cosmics. The relative normalization of the cosmic to beam halo template is allowed to float. Then we establish relative contributions of right to wrong vertex events by fitting events in the [-8, 1.2] ns window to the double Gaussian with the non-collision contribution subtracted.

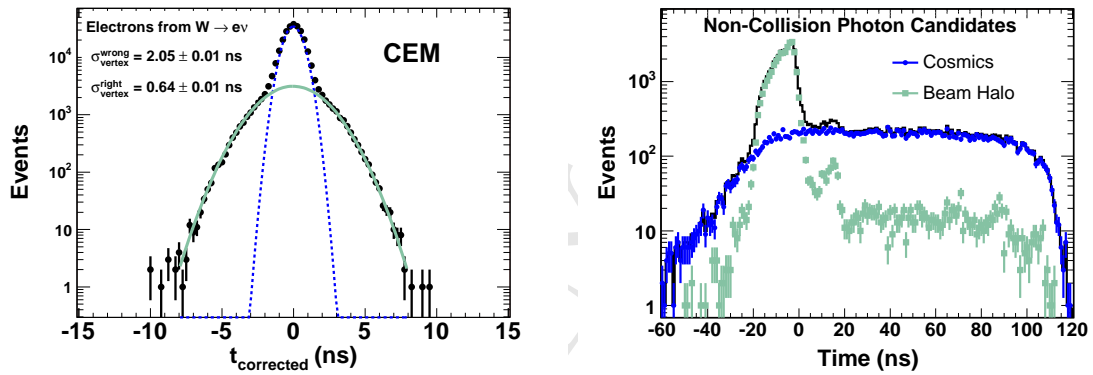


Figure 3: The background time shapes. The left-hand plot shows the expected timing distribution for collision photons, estimated using a sample of $W \rightarrow e\nu$ events, with the collision time subtracted estimated from data samples. The primary Gaussian is for the cases when the correct vertex is picked, the secondary Gaussian is for the cases when the wrong vertex is picked. The right-hand side shows photon timing from beam halo and cosmic ray background sources, estimated from data events with zero track activity.

4 Signal Monte Carlo

The signal acceptance is estimated using a GMSB model with the Snowmass slopes [4] simulated with Pythia as well as a full detector simulation. In this scenario a $\tilde{\chi}_1^0$ is NLSP and decays into a photon and a \tilde{G} , which is the lightest supersymmetric particle with a lifetime in the $O(1 \text{ ns})$ range. We include all possible processes, not only the two leading ones shown in Figure 1.

The acceptance depends on the $\tilde{\chi}_1^0$ lifetime and mass [7]. Heavy $\tilde{\chi}_1^0$ produces a photon at more extreme angles that translates into a photon having larger delay. Highly boosted $\tilde{\chi}_1^0$, more prominent at light masses, on the other hand, produces a photon flying in the original direction, thus making it indistinguishable from the prompt photons. The acceptance also drops as a function of the $\tilde{\chi}_1^0$ lifetime as more and more particles start decaying outside the detector. For reference, the total signal acceptance is $7.3 \pm 0.7\%$ for the GMSB point of the neutralino mass $m_\chi = 93.6 \text{ GeV}$ and lifetime $\tau_\chi = 10 \text{ ns}$. The biggest systematic error contribution comes from the photon ID efficiency and on the mean of the timing distribution. The list of the systematic effects on the acceptance can be found in Table 2

The final cut on the corrected time of arrival of the photon is selected to maximize the signal sensitivity based on the expected number of events from background estimation as shown in Figure 4. We note for completeness that the final set of kinematic requirements, shown in Table 1, are also optimized.

Factor	Systematic Uncertainty (%)
Time distribution and vertex selection	6.7
Photon ID efficiency	5.0
Jet energy	1.0
ISR/FSR	1.5
PDF	1.1
Total	8.6

Table 2: Summary of the systematic uncertainties for an example GMSB point at $\tilde{\chi}_1^0$ mass 93.6 GeV and lifetime of 10 ns. As a total we take a conservative 10%.

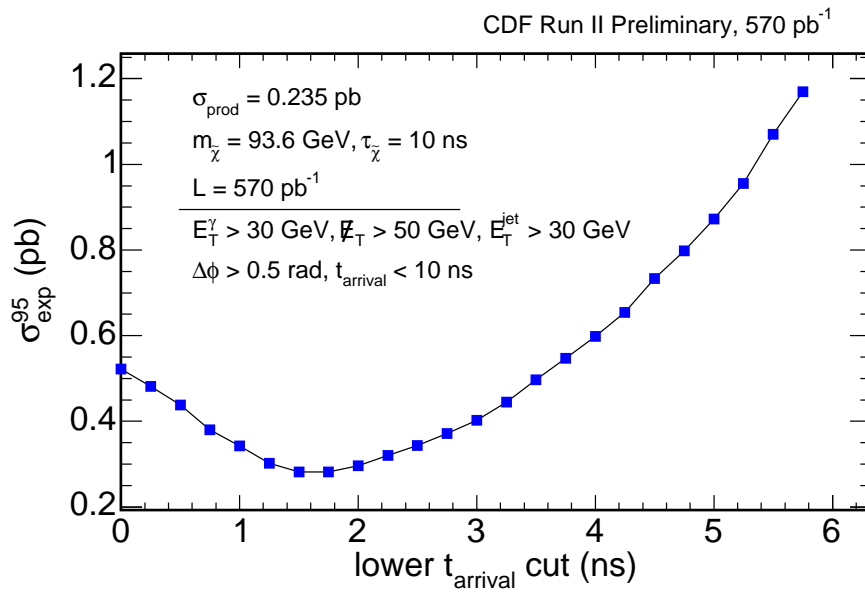


Figure 4: The expected 95% C.L. cross section limit as a function of the cutoff on the photon arrival time.

5 Results

After estimating all backgrounds in the timing window of $[1.5, 10]$ ns we open this previously blinded region and find 10 events. The number of expected events from all backgrounds is 7.6 ± 1.9 events; 4.7 ± 1.7 expected from collision photons and 2.9 ± 0.9 expected from non-collision sources. The total systematic error on the prediction is dominated by the uncertainty on the collision Gaussian parameters. A comparison between data and background as a function of the photon arrival time is shown in Figure 5. Other kinematic distributions are shown in Figure 6, indicating that the data is well-modeled by the background only hypothesis.

The result is consistent with no signal hypothesis, therefore we set limits on the neutralino lifetime and mass. Example cross section limits as a function of mass and lifetime are shown in Figure 7. The two dimensional exclusion region, taking into account the predicted production cross section, is shown in Figure 8. Since the number of observed events is slightly above expectations, the observed limits are slightly worse than the expected limits.

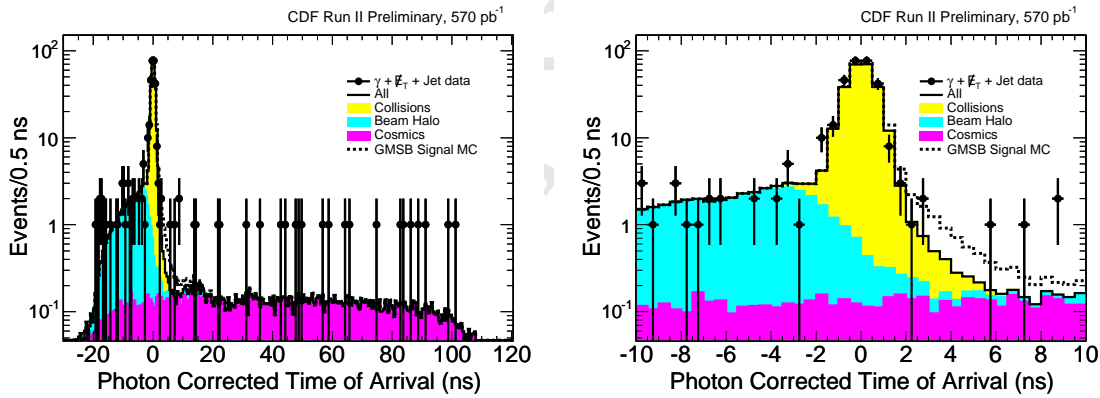


Figure 5: The predicted time distribution in the signal region for photons after all kinematic cuts. The right-hand side shows the same distributions, but for the region around the final signal region of $1.5 < t_{corrected} < 10$ ns. We compare the background prediction for the signal and the GMSB signal, for an example point at $m_{\chi} = 93.6$ GeV and $\tau_{\chi} = 10$ ns. We predict 7.6 ± 1.9 background events. The Monte Carlo is normalized to the number of expected signal events of 6.8 ± 0.7 .

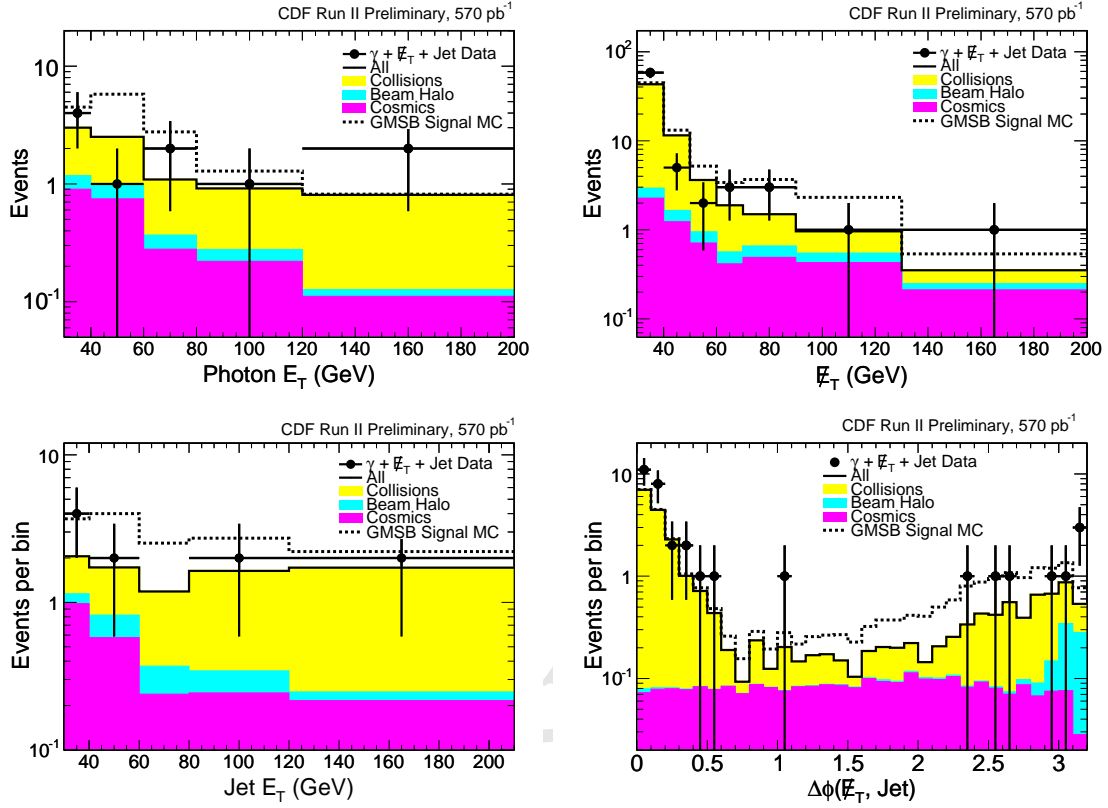


Figure 6: A comparison of the kinematic variables for the backgrounds, data and expected signal shapes. Note that all the distributions are well modeled by the data, indicating no evidence of new physics. Also note, that the final E_T cut is pushed from the 30 GeV cut indicated in the top right figure (trigger threshold) to 50 GeV in the final analysis; all other plots assume $E_T > 50$ GeV.

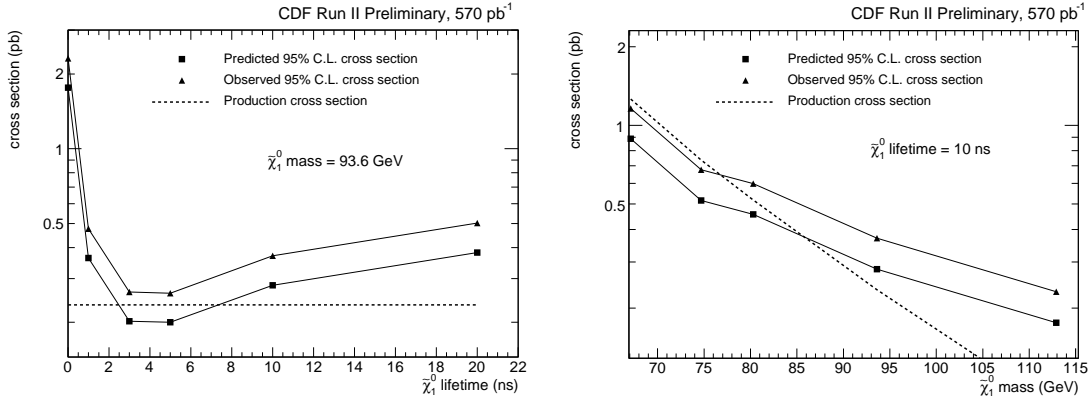


Figure 7: The expected and observed 95% C.L. cross section limit as a function of the $\tilde{\chi}_1^0$ mass (right) and lifetime (left) in our GMSB model.

2006

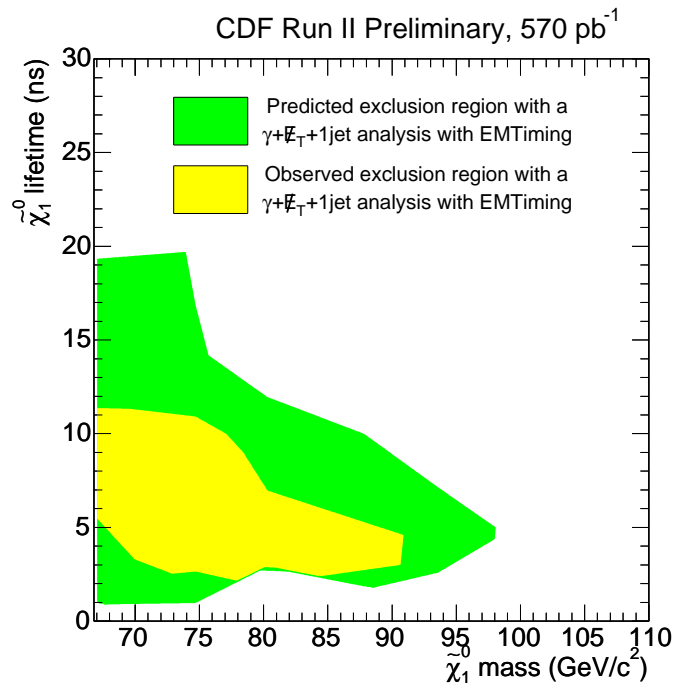


Figure 8: The exclusion region as a function of $\tilde{\chi}_1^0$ lifetime and mass. We show the exclusion region for the predicted and the observed number of background events.

DRAFT

References

- [1] S. P. Mertin, arXiv:hep-ph/9709356
- [2] J. L. Feng, A. Rajaraman, B. T. Smith, S. Su, and F. Takayama, arXiv:hep-ph/0410178
- [3] M. J. Strassler and K. M. Zurek, arXiv:hep-ph/0605193
- [4] See for example S. Ambrosanio, G. L. Kane, G. D. Kribs, S. P. Martin and S. Mrenna, Phys. Rev. D **54**, 5395 (1996) or C. H. Chen and J. F. Gunion, Phys. Rev. D **58**, 075005 (1998).
- [5] M. Goncharov et al., physics/0512171, accepted for publication in NIM. <http://hepr8.physics.tamu.edu/hep/emtiming/>
- [6] ALEPH Collaboration, A. Heister *et. al.*, Eur. Phys. J. C **25**, 339 (2002); A. Garcia-Bellido, Ph.D. thesis, Royal Holloway University of London, 2002 (unpublished), arXiv:hep-ex/0212024.
- [7] D. Toback and P. Wagner, Phys. Rev. D **70**, 114032 (2004).
- [8] We follow B. C. Allanach *et. al.*, Eur. Phys. J. C **25**, 113 (2002), and take the messenger mass scale $M_M = 2\Lambda$, $\tan(\beta) = 15$, $\text{sgn}(\mu) = 1$ and the number of messenger fields $N_M = 1$. The parameters c_{Grav} (gravitino mass factor) and Λ (supersymmetry breaking scale) are allowed to vary.